

Slow Manifolds in Chemical Kinetics

¹Muhammad Shahzad*, ¹Ibrar ul Haq, ¹Faisal Sultan, ¹Abdul Wahab, ²Faiz Faizullah and ³Ghaus Ur Rahman

¹Department of Mathematics, Hazara University, Mansehra, Pakistan.

²Department of BS and H, College of EME, NUST, Pakistan.

³Department of Mathematics and Statistics, University of Sawat, Pakistan.

shahzadmaths@hu.edu.pk*

(Received on 11th May 2015, accepted in revised form 17th June 2016)

Summary Modelling the chemical system, especially for complex and higher dimensional problems, gives an easy way to handle the ongoing reaction process with respect to time. Here, we will consider some of the newly developed computational methods commonly used for model reductions in a chemical reaction. An effective (simple) method is planned to measure the low dimensional manifold, which reduces the higher dimensional system in such a way that it may not affect the precision of the whole mechanism. The phase flow of the solution trajectories near the equilibrium point is observed while the initial approximation is measured with the spectral quasi equilibrium manifold, which starts from the equilibrium point. To make it an invariant curve, the approximated curve is first refined a certain number of times using the method of invariant grids. The other way of getting the reduced data in the low dimensional manifold is possible through the intrinsic low dimensional manifold. Then, we compare these two invariant curves given by both the methods. Finally, the idea is extended to the higher dimensional manifold, where more number of progress variables will be added.

Keywords: Chemical kinetics, Chemical equilibrium, Lyapunov function, Invariant manifolds, Model reduction.

Introduction

The mystery of chemistry could be understood if we know the details of the chemical mechanism. But the details of the mechanism involve a large number of chemical species c (microscopic point of view), which are difficult to measure in a few steps. Therefore, it is important to model the system on a macroscopic scale, such as the system must be defined by its position and velocity for each induced chemical (species) of the system. Also, in a thermodynamic system, it is necessary to know about the pressure and temperature, etc. Some studies suggest that in the case of thermodynamic equilibrium, it is observed that there is no change at the macroscopic level; however, some changes took place on the microscopic level.

Now, if such variations occur at each stage of the ongoing process of the chemical mechanism (even before reaching its equilibrium state), it is important to know its relaxation time and behaviour of the induced species during the transition process in the final stage.

Our aim is to design a kinetic model to derive the reaction mechanism, which remains vital for the whole mechanism. The acquired data from the new reduced system is then simulated in such a way that it may not affect the accuracy. For

basic notation and representation, we follow these assumptions:

Reaction Mechanism

A single or a multiple steps reversible chemical reaction can be usually represented as:



Here, α_i, β_i (≤ 3) are the stoichiometric coefficients. Reactants and products involved in the chemical reactions are represented by c_{A_i} and their total numbers are represented by N_A, N_B . n -dimensional stoichiometries vector γ_i of the reaction (1) are defined as:

$$\gamma_i = \beta_i - \alpha_i \quad (2)$$

Stoichiometries vectors generate the stoichiometries matrices having dimensions $(N_{or} \times N_c), N_{or}$ that stands for the number of overall reactions while N_c represents the number of species (chemical) involved in the system. Similarly, the molecular matrix having dimension $(N_c \times N_e)$ shows the composition of the chemical substances, where N_e are the number of chemical elements.

*To whom all correspondence should be addressed.

In the case of simultaneous or complex chemical reactions, it is better (both from an academic as well as a practical point of view) to reduce the system to its dimension. Thus, according to Gibbs rule, we can find the (minimum) number of key components N_{kc} required to explain the chemical reactions, which is:

$$N_{kc} = N_c - N_e \quad (3)$$

The rate of reaction at each elementary step is the difference between its forward and backward rate, *i.e.* $w = w_i^+ - w_i^-$. When the system moves towards equilibrium then $w = 0$ and we have $w_i^+ = w_i^-$ but it is important to mention here, it is the (forward and backward) rate of reaction that are equal while concentrations of reactants and products are not equal [1]. According to the law of mass action, the rate depends on concentration and rate coefficients

$$w_i^+ = k_i^+ \prod_{i=1}^{N_A} c_{A_i}^{\alpha_i}, \quad w_i^- = k_i^- \prod_{i=1}^{N_B} c_{A_i}^{\beta_i}, \quad (4)$$

i.e., k_i^+ is the rate coefficient for a forward while k_i^- is related to backward reactions and their ratio $k_i^+ / k_i^- = k_{eq}$ represents equilibrium constants. As an intensive variable $c_i = \frac{N_i}{V}$ ($V > 0$ Volume), the vector $c = \frac{N}{V}$ is a vector of concentration while $N_i \in C_{A_i}$ is an extensive variable. The kinetic equations for a system (without external flux) will become

$$\frac{dN}{dt} = V \sum_{i=1}^n \gamma_i w_i(c), \quad \dot{N} = VK(c), \quad K(c) = \sum_{i=1}^n \gamma_i w_i(c).$$

In case of isothermal and isochoric process, an extra condition exists in the form of $T, V = (\text{constant})$. Therefore, the above system finally takes a form:

$$K(c) = \frac{dc}{dt} = \sum_{i=1}^n \gamma_i w_i(c), \quad (5)$$

Now considering the law of conservation of atoms, which plays an important role in the reduction of the complex chemical system, are also taken into account in the form of linear constraints, *i.e.*,

$$Mc = Cnt. \quad (6)$$

Quasi and Spectral Quasi Equilibrium Manifold

The quasi equilibrium manifold (QEM) depends on two entities [2], Entropy and Slow variables. Entropy is basically a Lyapunov function and G plays an important role for its stability while the convergence of the system obeys the 2nd law of thermodynamics [3, 4]. Slow variable means a differentiable function of a variable c with an assumption of small fast-slow projection.

$$G = \sum_{i=1}^n c_i \left[\ln\left(\frac{c_i}{c_i^{eq}}\right) - 1 \right]. \quad (7)$$

Now, we define the QEM in term of conditions, *i.e.*

$$G \rightarrow \min, \quad (m, c) = \eta, \quad Mc = Cnt. \quad (8)$$

Here m_i are n -dimensional vectors, η values are the reduced description of the species in a situation and we are left with the $N_c - N_e$ degree of freedom. If m_i is selected as the i th-left slowest eigenvector of the Jacobean $L(c) = \frac{\partial K(c)}{\partial c_i} \Big|_{c^{eq}}$ corresponding to small absolute eigenvalues $|\lambda_i|$, the solution obtained from (8) is known as Spectral Quasi Equilibrium Manifold (SQEM) (for more details see [5-9]).

Now, in the next step, we will project this initial solution onto the constructed slow manifold in order to split the motions into slow and fast. The operator P_T (thermodynamic projector) projects the vector field at each point of the manifold in the tangent space to give the induced vector field $P_T K(c)$, which defines the "slow and fast motions" duality [6]. Therefore, projector depends on two things: tangent space of the manifold Ω and concentration point c . Now the differential of a linear function G , and induced vector field are:

$$DG(c) = (\nabla G(c), c).$$

$$DG(P_T K(c)) \leq 0, \quad \forall c \in \Omega.$$

The projector P_T obeys the condition given above if the following condition is satisfied, *i.e.*

$$\ker(P_T) \subset \ker(DG(c)), \quad \forall c \in \Omega$$

∇ is Gradient of the function, *i.e.* $\nabla G = \ln(c_i / c_i^{eq})$ and $H = \partial^2 G / \partial c_i \partial c_j$ is the second derivative matrix of G . \ker is the null space of the operator. An entropy scalar product $\langle \cdot, \cdot \rangle$ is defined as $\langle c_p, c_{p+1} \rangle = (c_p, Hc_{p+1})$, while (\cdot, \cdot) implies Euclidean scalar product.

Manifold for Grid Construction

By using the SQEM method, we will measure the one dimensional curve starting from any point c_p (or equilibrium) that lies over it. We can measure the next point by adding a shift hc_p , $c_{p+1} = c_p + hc_p$ and $hc_p = \sum_{i=1}^z \rho_i v_i$ (9)

Thus, all the possible outcomes can be obtained c_{p+n} in the same manner. v_i is the unknown variable, which we have to find while ρ is the basis of null space of the matrix M having a dimension $Z = \dim(N_c - N_e)$. The line ℓ lies between c_{p+1} and c_p having a parametric form $c = \varphi t + c_{p+1}$, whereas t is a vector of T (tangent space) spanning ℓ and φ is taken as a parameter.

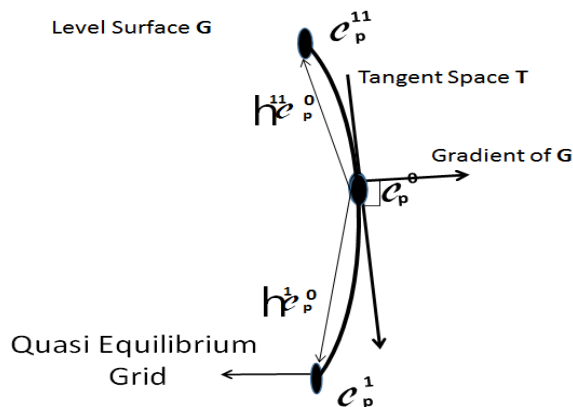


Fig. 1: The general idea of grid construction and its variation from one grid to the next grid point.

Now, applying the method of SQEM; first, the constraints (linear) of QEM can be

rewritten in the form:
$$E = \begin{bmatrix} m_1 \\ \vdots \\ \ddot{m}_q \\ M \end{bmatrix}$$

Here $m_1 \dots m_q$ are the reduced variable vectors from single to higher dimensions. Then, the dimension of basis t_j in $\ker(E)$ will be $(z-q)$ and the system will be:

$$\sum_{i=1}^z \langle t_j, \rho_i \rangle v_i = -\langle t_j, \nabla G(c_p) \rangle, \quad \forall j = 1, \dots, z-1$$

$$\sum_{i=1}^z (m, \rho_i) v_i = 0, \quad \|hc_p\| = \delta^2. \quad (10)$$

The solution of the above system (10) delivers two real solutions at each grid point as shown in Fig. 1. In our case, we will start measuring from c^{eq} (equilibrium point) with the selection of slowest first variable vector m_1 among the available q vectors to solve the system (10). In this way, we obtain first initial SQEM given by grid nodes. This initially approximated curve is then refined in a node-by-node process to find out the invariant manifold by using any appropriate method like the method of the invariant grid (MIG) [10, 11]. After that, out of the remaining $q-1$ available vectors, we take the second m_2 and get some more combinations of nodes or in simple words, another SQEM curve passing through c^{eq} . The second curve can also be refined through the same process to make it an invariant curve. Similarly, the idea is extendable to the q th step in order to find out all the possible combinations of vectors. The same idea is used to construct the higher dimensional manifold and it is illustrated with an example in the next section.

Experimental

Here we consider some chemical reactions defined over a closed system [12]. The reaction mechanism involves a three-step reversible oxidation mechanism (B_2 as oxygen) with four chemical species, *i.e.* $A = c_1, B_2 = c_2, AB = c_3, AB_2 = c_4$.

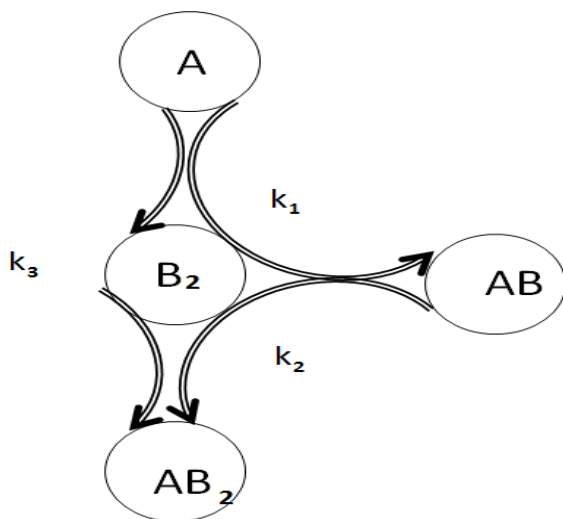
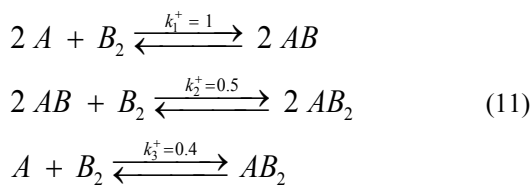


Fig. 2: Example of three step reversible reactions involves four chemical species. In the first step, A reacts with B_2 and it is transformed into AB . In the second step; AB reacts with B_2 and produces AB_2 while A also produces AB_2 when it reacts with B_2 . Here, k_i indicates the rate coefficients for the first, second and third reaction steps.



The system shown above (11) delivers the stoichiometries vector and matrix S w.r.t (2), while the molecular matrix M is given by (6) in matrix form.

$$S = \begin{pmatrix} -2 & -1 & 2 & 0 \\ 0 & -1 & -2 & 2 \\ -1 & -1 & 0 & 1 \end{pmatrix} \quad M = \begin{pmatrix} 1 & 0 \\ 0 & 2 \\ 1 & 1 \\ 1 & 2 \end{pmatrix} \begin{matrix} A \\ B_2 \\ AB \\ AB_2 \end{matrix} \tag{12}$$

The involved species are mentioned above in S while these species are in a row in M and elements are in its columns above. The relation between these matrices can be easily mentioned as $S^M (N_{sp} \times N_e) = 0$. Whereas according to equation (3), we have $N_{lc} = 2$ for (11).

Similarly, the system of kinetic equations can be solved by using the relation (5), i.e.

$$K(c) = \begin{bmatrix} -k_3c_1c_2 + k_3c_4 - 2k_1c_1^2c_2 + 2k_1c_3^2 \\ -k_3c_1c_2 + k_3c_4 - k_2c_2c_3^2 + k_2c_4^2 - k_1c_1^2c_2 + k_1c_3^2 \\ -2k_2c_2c_3^2 + 2k_2c_4^2 + 2k_1c_1^2c_2 - 2k_1c_3^2 \\ k_3c_1c_2 - k_3c_4 + 2k_2c_2c_3^2 - 2k_2c_4^2 \end{bmatrix} \tag{13}$$

and its Jacobean $L(c^{eq})$ can be measured as:

$$L(c^{eq}) = \begin{bmatrix} -0.240 & -0.700 & 0.500 & 0.050 \\ -0.140 & -0.470 & 0.230 & 0.060 \\ 0.200 & 0.460 & -0.540 & 0.020 \\ 0.040 & 0.240 & 0.040 & -0.070 \end{bmatrix} \tag{14}$$

Now, in the case of SQEM, the choice of selecting the slowest vector will not be directly done from L the way it was done in QEM [5]. Therefore, the first and second slowest left eigenvectors x_1^{sl} , $x_2^{sl}(m_{1,2})$ of the Jacobian matrix

$$\{L = \frac{\partial K_i}{\partial c_j} |_{c^{eq}}\} \text{ will become:}$$

$$m = \begin{cases} x_1^{sl} = [-0.0313 & -0.7405 & -0.5839 & 0.3311] \\ x_2^{sl} = [0.2694 & 0.7689 & -0.5779 & -0.0478] \end{cases}$$

By using the slow vector scheme, we will measure lower dimensional manifold (LDM).

Results and Discussion

By solving (10) in quasi equilibrium grid nodes, we start measuring from equilibrium point $c_0 = c^{eq}$. Adding a shift vector hc_p we first move towards the left branch $c_{p+1} < c_p$ and get new grid points $c_{p+1} = c_p + hc_p$. Similarly, we impose the condition of $c_{p+1} > c_p$ in order to calculate new grid points of the right branch. The process of obtaining a new grid point will continue until we reach its maximum and minimum values as explained in Fig. 3.

On the other side, we sketch the graph of our reduced systems with respect to time and observe steady state behavior in Fig. 4 along with their convergence towards its equilibrium after starting with different initial points Fig. 5.

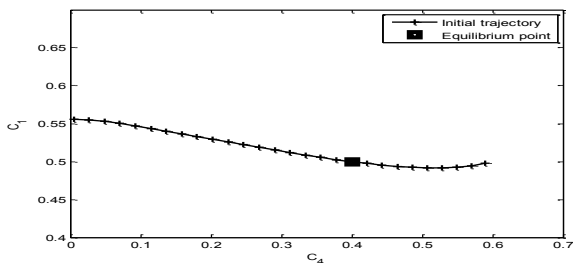


Fig. 3: D-SQE grids measurement starting from the equilibrium point (square) to its right and left branch whereas $\delta^2 = 10^{-3}$ and $m = x_1^{sl}$ is taken.

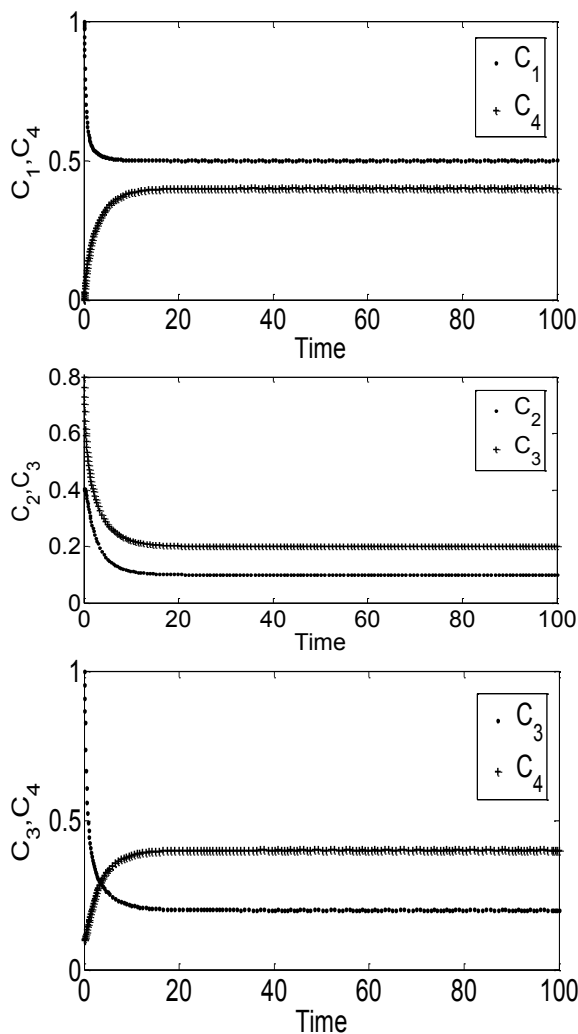
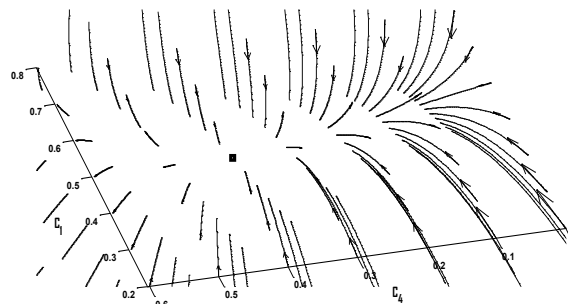
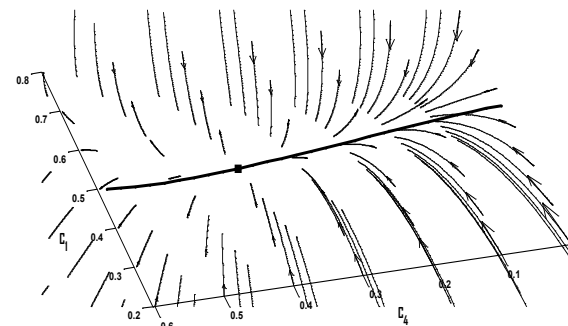


Fig. 4: The figures shown here represent the concentration C_i versus time relationship for the synthesis of CO_2 . The steady state behavior is observed in the case of its reduced form (c_1, c_4) , (c_2, c_3) , (c_3, c_4) from the system (2). Note that after completing the transition period, the system moves towards steady state or equilibrium.



(a)

Fig. 5a: Phase flow of the solution trajectories (in its reduced form c_1, c_4) near the equilibrium point (square) is observed after starting through different initial points.



(b)

Fig. 5b: An approximated SQEM (solid line) passes through the equilibrium point (square), which gives the idea of LDM, where the phase flow of the solution trajectories (in its reduced form c_1, c_4) approaches the equilibrium point and then it moves along it.

Now, the sketch of our problem gives a clear view of the manifold based on slow motion assessment Ω_{slow} that according to the initial condition, the system moves to the neighborhood of the manifold and then it moves along the manifold [6]. A sub-manifold $\varpi \in \Omega$ defined in some domain will be invariant if its solution trajectory $c(t)$ starting on it $c(t_0) \in \varpi$ never leaves the system throughout its time $t > t_0$ while moving along $c(t) \in \varpi$ [13, 14].

Although our initial approximation is away from the actual (not exact) curve, this error can be removed by refining the solution curve. Therefore, we apply the MIG and get the refined curve Fig. 6.

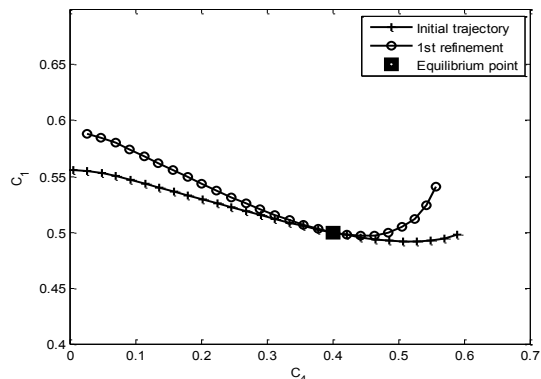


Fig. 6: Initially approximated SQE-grids are first refined with the MIG by keeping $\epsilon^2=10^{-3}$ and started from equilibrium.

Now, the initially approximated solution, given by SQEM, is refined by the MIG (Fig. 6), but still, we cannot claim that this is the final or the exact solution curve; therefore, we will refine it further. But it is still unclear how long we can go for it. In our case (1), we get an invariant curve after refining the initial solution curve three times Fig. 7a. On the other side, we have observed that the method, defined by Mass and Pope [15-17] (Intrinsic low dimension manifold ILDM) and applied by many authors [18-20] based on slow eigenspace, will find out the best solution in its first calculation Fig. 7b.

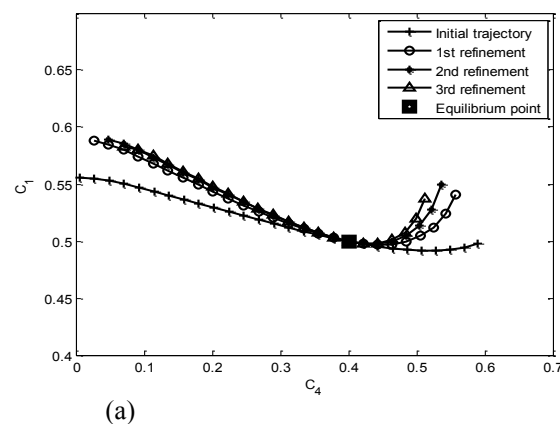


Fig. 7a: An invariant manifold has been measured by refining (with MIG) the initial approximated SQEM three times.

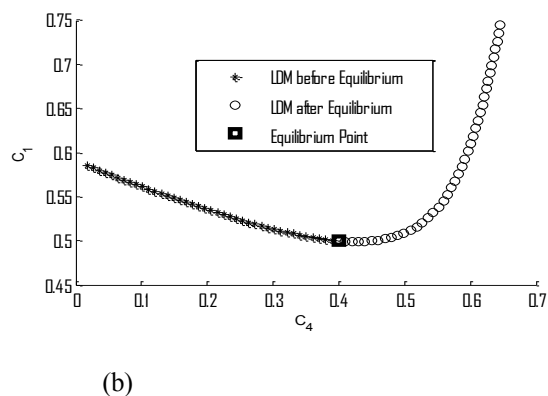


Fig. 7b: The initial curve is measured by the method of intrinsic low dimensional manifold starting from the equilibrium point on both sides.

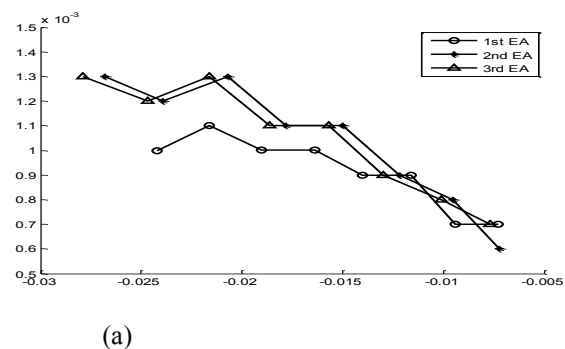


Fig. 8a: Error Analysis (EA) of the measured curves given by MIG shows the variation in grid points during its first, second and third refinements.

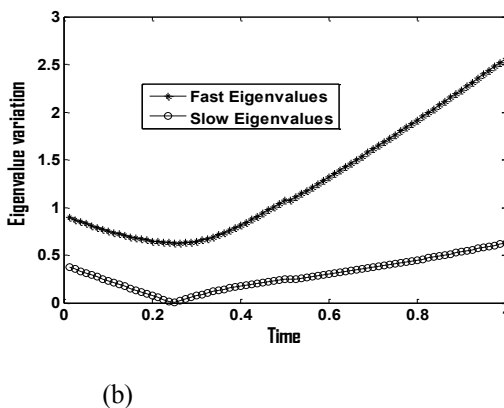


Fig. 8b: During the measurement of the lower dimensional manifold with respect to ILDM, the absolute eigen values at each grid point have been plotted with respect to time.

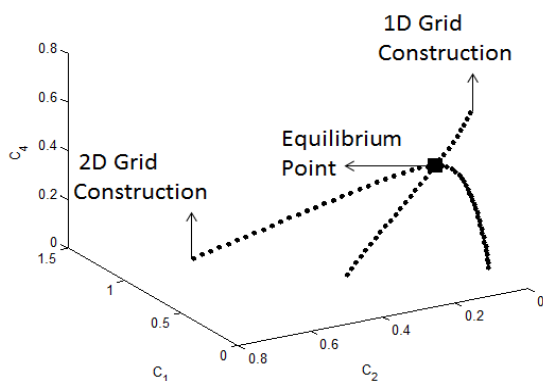
Table-1: The above table shows the difference (positive) between the initial (I) and refined (R) values of the eight grid point, which are presented in Fig. 8a.

Fig. 8a.	I-R1	I-R2	I-R3
1	0.0242	0.0268	0.0247
2	0.0216	0.0239	0.0216
3	0.0190	0.0207	0.0186
4	0.0164	0.0178	0.0157
5	0.0140	0.0150	0.0130
6	0.0116	0.0122	0.0101
7	0.0094	0.0095	0.0077
8	0.0073	0.0072	0.0053

Higher Dimension

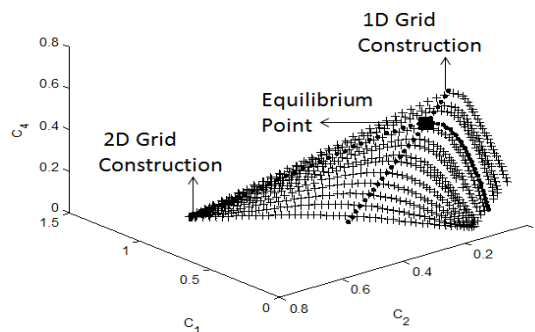
Now, after measuring an invariant curve, we extend the idea for the higher dimensional manifold. This means we have to add more number of progress variable (chemical species). The idea is similar to the procedure adopted for one dimensional curve measured within the first slowest eigen spaces, while for two dimensional curves, the second slowest eigen space must also be taken into account.

Therefore, the procedure starts from the equilibrium point and divides into two subsequent processes. Initially, the system (10) was resolved for $m_1 = x_1^{st}$ and an invariant curve is obtained after being refined at each grid point shown in Fig. 9a. Then in the second step, we solve the system again but keeping $m_2 = x_2^{st}$ over the refined grid point of the 1D curve as shown in Fig. 9b. In both the cases, we take $\varepsilon^2 = 10^{-3}$. In the same manner, this idea is further extendable to higher dimensions.



(a)

Fig. 9a: The 1D, LDM curve is further extended to 2D with the addition of other progress variable passing through equilibrium point.



(b)

Fig. 9b: For 2D grid construction, we measure the LDM at each grid point of the 1D curve.

Conclusion

In this paper, we have presented the idea to measure a low dimensional manifold for the system of complex chemical reaction through analytical and computational techniques. The model reduction is done through best available modern techniques (SQEM, ILDM) along with the comparison of their results. Although the initial curve (*i.e.* SQEM) is far away from the exact solutions, we are able to get an invariant solution curve through proper algorithm and refinement with MIG. While doing error analysis of each grid point, we are able to see the refinement at each step. Our construction strategy is based on a geometrical approach depending on finding and examining the dynamic behaviour of all the induced (or participate) species in the system. By using the same approach, we are able to explain the behavior of the solution trajectories near the equilibrium point and their approach towards and after the equilibrium. In the end, we have added a new progress variable to show that in a complex system, required dimensional curves can easily be constructed. By combining all the results, we have shown how the reacting species behave in the whole mechanism.

Reference

1. G. V. Yablonskii, V. Bykov, V. Elokhin and A. Gorban, Kinetic Models of Catalytic Reactions, Elsevier, (1991).
2. M. Shahzad, PhD Thesis, *Slow Invariant Manifold and its Approximations in Kinetics of Catalytic Reactions*, University of Leicester, Leicester, (2011).

3. A. N. Gorban, P. A. Gorban and G. Judge, Entropy: the Markov Ordering Approach, *Entropy*, **12**, 1145 (2010).
4. A. N. Gorban, M. Shahzad, The Michaelis-Menten-Stueckelberg Theorem, *Entropy*, **13**, 966 (2011).
5. E. Chiavazzo, A. N. Gorban, I. V. Karlin, Comparison of Invariant Manifolds for Model Reduction in Chemical Kinetics, *Commun. Comput. Phys.*, **2**, 964 (2007).
6. A. N. Gorban and I. V. Karlin, *Entropy, Quasiequilibrium, and Projectors Field*, Springer, (2005).
7. M. Shahzad, H. Arif, M. Gulistan and M. Sajid, Initially Approximated Quasi Equilibrium Manifold, *J.Chem.Soc.Pak*, **37** (2015).
8. M. Shahzad, S. Rehman, R. Bibi, H.A. Wahab, S. Abdullah, S. Ahmed, Measuring the complex behavior of the SO₂ oxidation reaction, *Computational Ecology and Software*, **5** (2015).
9. M. Shahzad, F. Sultan, I. Haq, H.A. Wahab, M. Naeem and F. Haq, Computing the Low Dimension Manifold in Dissipative Dynamical Systems, *The Nucleus*, **53**, (2016).
10. A. N. Gorban and I. V. Karlin, Invariant Manifolds for Physical and Chemical Kinetics, Lect. Notes Phys, Springer Berlin Heidelberg, 660 (2005).
11. A. N. Gorban, I.V. Karlin, Method of invariant manifold for chemical kinetics, *Chemical Engineering Science*, **58**, 4751 (2003).
12. G. Marin and G. S. Yablonsky, *Kinetics of Chemical Reactions*, John Wiley and Sons, (2011).
13. A. N. Al-Khateeb, J. M. Powers, S. Paolucci, A. J. Sommesse, J. A. Diller, J. D. Hauenstein, J. D. Mengers, One-Dimensional Slow Invariant Manifolds for Spatially Homogenous Reactive Systems, *J. Chem. Phys.*, **131**, 024118 (2009).
14. E. Chiavazzo, Ph.D Thesis, *Invariant Manifolds and Lattice Boltzmann Method for Combustion*, in, Diss., Eidgenössische Technische Hochschule ETH Zürich, (2009).
15. U. Maas, Efficient Calculation of Intrinsic Low-Dimensional Manifolds for the Simplification of Chemical Kinetics, *Computing and Visualization in Science*, **1**, 69 (1998).
16. U. Maas, S. B. Pope, Simplifying Chemical Kinetics: Intrinsic Low-Dimensional Manifolds in Composition Space, *Combust Flame*, **88**, 239 (1992).
17. U. Maas and S. B. Pope, Implementation of Simplified Chemical Kinetics Based on Intrinsic Low-Dimensional Manifolds, in: Symposium (International) on Combustion, **24**, 103 (1992).
18. R. E. Petrosyan, Ph.D Thesis, *Developments of the Intrinsic Low Dimensional Manifold Method and Application of the Method to a Model of the Glucose Regulatory System*, University of Notre Dame, (2003).
19. O. Gicquel, D. Thevenin, M. Hilka and N. Darabiha, Direct Numerical Simulation of Turbulent Premixed Flames Using Intrinsic Low-Dimensional Manifolds, *Combustion Theory and Modelling*, **3**, 479 (1999).
20. H. Bongers, J. Van Oijen and L. De Goey, Intrinsic Low-Dimensional Manifold Method Extended with Diffusion, *Proceedings of the Combustion Institute*, **29**, 1371 (2002).